



**HAL**  
open science

## Usefulness of the Interface Fresnel zone for simulating the seismic reflected amplitudes

Nathalie Favretto-Cristini, Paul Cristini, Eric de Bazelaire

► **To cite this version:**

Nathalie Favretto-Cristini, Paul Cristini, Eric de Bazelaire. Usefulness of the Interface Fresnel zone for simulating the seismic reflected amplitudes. 2006. hal-00110267

**HAL Id: hal-00110267**

**<https://hal.science/hal-00110267>**

Preprint submitted on 27 Oct 2006

**HAL** is a multi-disciplinary open access archive for the deposit and dissemination of scientific research documents, whether they are published or not. The documents may come from teaching and research institutions in France or abroad, or from public or private research centers.

L'archive ouverte pluridisciplinaire **HAL**, est destinée au dépôt et à la diffusion de documents scientifiques de niveau recherche, publiés ou non, émanant des établissements d'enseignement et de recherche français ou étrangers, des laboratoires publics ou privés.

# Usefulness of the Interface Fresnel zone for simulating the seismic reflected amplitudes

Nathalie Favretto-Cristini<sup>1</sup> and Paul Cristini<sup>1</sup> and Eric de Bazelaire<sup>2</sup>

October 11, 2006

<sup>1</sup>Centre National de la Recherche Scientifique, Laboratoire de Modélisation et Imagerie en Géosciences (UMR 5212), Université de Pau et des Pays de l'Adour, BP 1155, 64013 Pau Cedex, France. Contact author: nathalie.favretto@univ-pau.fr

<sup>2</sup>11 route du Bourg, 64230 Beyrie-en-Béarn, France

## Keywords

Fresnel volume, Interface Fresnel zone, amplitude, reflected wave, P-wave, smooth interface.

## Short title

Usefulness of the IFZ for wave amplitude

## Abstract

The aim of the paper is to emphasize the importance of accounting for the Fresnel volume (FV) and for the Interface Fresnel zone (IFZ) for simulating the amplitudes of the spherical waves reflected from an interface between elastic media and recorded at the receiver. For this purpose, by considering the problem of interest as a problem of diffraction by the IFZ, we have developed a method which combines the Angular Spectrum Approach (ASA) with the IFZ concept to get the 3D analytical solution. The comparison between the amplitude-versus-angle curve predicted by our approximation with that predicted by the classical plane-wave theory, and also with the exact solution, clearly enlightens three points. First, for specific regions of incidence angles, for which the geometrical-spreading compensation is not sufficient anymore to reduce the point-source amplitudes to the plane-wave amplitudes, the additional application of the FV and of IFZ concept is necessary. Second, as our approximation is concerned only with the reflected wave, its predictions fit well the exact solution, provided there is no interference between the reflected wave and the head wave. Third, they exhibit oscillations in the postcritical region which result from the interference of the IFZ with the sharp edge of the reflection coefficient.

## Introduction

Since many decades geophysicians have developed various theoretical methods to fit the real seismic data, their ultimate goal being to invert them to retrieve the geometrical and physical characteristics of the Earth. Since the media heterogeneity can be highly complex, depending on the seismic frequency range of interest, using the exact form (in the time domain) of waves emanating from a point source and being reflected by interfaces (Aki & Richards, 2002, chapter 6) can be a very difficult task for interpreting some seismic observations. Interpretation of such observations then always relies on approximations.

The basis of many seismic studies is the geometrical ray theory (Cerveny, 2001). Under this approximation it is assumed that the high-frequency part of elastic energy propagates along infinitely narrow lines through space, called rays, which join the source and the receiver. Ray theory is then strictly valid only in the limit of a hypothetical infinite-frequency wave. As recorded data have a finite frequency content, it is accepted that seismic wave propagation is extended to a finite volume of space around the geometrical ray path, called the 1<sup>st</sup> Fresnel volume (Kravtsov & Orlov, 1990), hereafter denoted FV. The wave properties are thus influenced not only by the media structure along the ray, but also by the media structure in the vicinity of the ray. This well-known limitation of ray theory has received broad attention in recent past years. The concept of FV (also known as physical ray, 3D Fresnel zone...) is continually being developed and has found so many applications in seismology and in seismic exploration, that it is impossible here to review all the books and articles which pay attention to it in seismic wave propagation. Nevertheless, we shall mention the works of Cerveny and his co-authors who have proposed two methods for including FV parameter calculations into the ray tracing procedure in complex 2D and 3D structures. The first one, called the Fresnel volume ray tracing (Cerveny & Soares, 1992), combines the paraxial ray approximation with the dynamic ray tracing and is only applicable to zero-order waves (direct, reflected and transmitted waves...), whereas the second method, more accurate and efficient than the previous one, is based on network ray tracing (Kvasnicka & Cerveny, 1994). Contrary to the previous methods, the FVs can also be computed without knowledge of the velocity model of the media (Hubral et al., 1993). Note that analytical expressions for FVs of seismic body waves and for their intersection with interfaces, called the Interface Fresnel zones (IFZ), have been derived in Kvasnicka & Cerveny (1996a) and in Kvasnicka & Cerveny (1996b). Many works have shed new light on the role of the FVs in the seismic imaging of reflectors. They have shown that, besides being connected with the resolution of seismic methods (Sheriff, 1980; Lindsey, 1989; Knapp, 1991), the FVs also play a role in the migration and demigration processes (Hubral et al., 1993; Schleicher et al., 1997). Moreover, FVs have been applied to inversion studies of seismic data (Yomogida, 1992) and they have been incorporated into tomographic traveltime inversion schemes (Vasco & Majer, 1993). Note also that in global seismology, sensitivity kernels have been developed for global tomography inversions to overcome the limitations of ray theory and to account for finite-frequency effects upon seismic wave propagation (Zhou et al., 2005). Sensitivity kernels (also known as Fréchet kernels) linearly relate velocity perturbations of the medium to changes in some seismic observables (traveltime, waveform, splitting intensity) of the band-limited waves (Marquering et al., 1999; Dahlen et al., 2000; Dahlen & Baig, 2002; Favier & Chevrot, 2003). FVs and sensitivity kernels are closely connected through the concept of constructive interferences of waves (Vasco et al., 1995; Spetzler & Snieder, 2004).

The variability of the amplitudes of the reflected waves, with the incidence angle, is of great interest for many seismological applications, for instance to constrain localization of reflectors

and media properties. Since the media heterogeneity can be highly complex in the typical seismic frequency range, and considering that both source and receivers are usually located far from the interfaces, the exact form of spherical waves generated by a point source is not convenient for interpreting complex seismic observations. A survey of the literature brings to light that most calculations are generally performed within the framework of monochromatic plane-wave (PW) theory or finite-frequency theory without nevertheless taking into account the frequency-dependent spatial regions (i.e., FVs) in the vicinity of the geometrical ray. This is justified by the fact that for some typical configurations and for subcritical incidence angles, the geometrical-spreading compensation is mostly quite sufficient to reduce the point-source amplitudes to the PW amplitudes. On the contrary, for critical and post-critical incidence angles, this compensation is generally not sufficient anymore, and an additional processing should be considered. To the best of the authors' knowledge, a theoretical study of the FV and IFZ imprint on the reflected wave amplitudes, for critical and postcritical angles, has not been developed yet, despite the band-limited nature of seismic data. This is the purpose and scope of this work.

The paper is organized in two sections. Section 1 is concerned with 3D analytical derivations. Firstly, special attention is paid to the FV and to the IFZ which are frequency-dependent and which also depend on the position of the source and the receivers. We reformulate the concept of the FV in order to derive the expression for the IFZ valid whatever the incidence angle. Secondly, we introduce the method we used for deriving the amplitude of the P-wave, emanating from the point source and recorded at the receiver after its reflection on a smooth interface between elastic media. As the problem under consideration can be viewed as a problem of diffraction by the IFZ, i.e. the physically relevant part of the interface which actually affects the reflected wavefield, we applied the Angular Spectrum Approach (ASA) (Goodman, 1996) to get the 3D analytical solution. Section 2 investigates the role of the FV and the IFZ in the reflected wave propagation in the critical and postcritical regions. The variation in the reflected P-wave amplitude, as a function of the incidence angle, evaluated with the ASA is compared with the PW reflection coefficient, and with the exact solution obtained with the 3D code OASES. The influence of the frequency bandwidth of the source on the wave amplitude is also investigated.

## 1 3D analytical derivations of the reflected P-wave amplitude

### 1.1 Characteristics of the Fresnel volume and of the Interface Fresnel Zone

We consider two homogeneous isotropic elastic media in welded contact at a plane interface situated at a distance  $z_M$  from the  $(\vec{x}, \vec{y})$ -plane including the point source S  $(x_S, 0, 0)$ , and the receiver R  $(x_R, 0, 0)$ . The source generates in the upper medium a spherical wave with a constant amplitude. The spherical wave can be decomposed into an infinite sum of PW, synchronous each other at the time origin. We consider the harmonic PW with frequency  $f$  which propagates in the upper medium with the velocity  $V_{P1}$  from S to R, after being reflected by the interface at the point M  $(x_M, 0, z_M)$  in a specular direction  $\theta$  with respect to the normal to the interface (Figure 1). Let the traveltime of the specular reflected wave be  $t_{SMR}$ .

The set of all possible rays  $SM_iR$  with constant traveltime  $t_{SMR}$  defines the isochrone for the source-receiver pair (S,R), relative to the specular reflection SMR. This isochrone describes an ellipsoid of revolution tangent to the interface at M, whose rotational axis passes through S and R. By definition, the FV corresponding to S and R, and associated with the reflection

at M, is formed by virtual points F which satisfy the following condition (Kravtsov & Orlov, 1990):

$$|t(F, S) + t(F, R) - t(M, S) - t(M, R)| \leq \frac{T}{2} \quad , \quad (1)$$

or:

$$|l(F, S) + l(F, R) - l(M, S) - l(M, R)| \leq \frac{\lambda_1}{2} \quad , \quad (2)$$

where  $\lambda_1 = \frac{V_{P1}}{f}$  is the wavelength corresponding to the dominant frequency  $f$  of the narrow-band source signal. The quantity  $t(X, Y)$  denotes the travelttime from the point X to the point Y, and  $l(X, Y)$  the distance between X and Y. The FV is then represented by the volume situated above the interface in the upper medium and bounded by two ellipsoids of revolution, with foci at S and R, tangent to parallel planes to the interface and situated at a distance  $\frac{\lambda_1}{4}$  beyond and above the interface. The two ellipsoids of revolution are defined by:

$$\frac{x^2}{\left(\frac{z_M}{\cos\theta} \pm \frac{\lambda_1}{4}\right)^2} + \frac{y^2}{\left(\frac{z_M}{\cos\theta} \pm \frac{\lambda_1}{4}\right)^2 - z_M^2 \tan^2\theta} + \frac{z^2}{\left(\frac{z_M}{\cos\theta} \pm \frac{\lambda_1}{4}\right)^2 - z_M^2 \tan^2\theta} - 1 = 0 \quad . \quad (3)$$

Here, it must be precised that, as seismic wavefields are transient and large-band, it is generally necessary to decompose the source signal into narrow-band signals for which monochromatic FV can be constructed for the prevailing frequency of the signal spectrum (Knapp, 1991). The physical meaning of eq.2, describing the FV concept, is quite obvious: the waves passing through the diffraction points F interfere constructively with the specular reflected wave when the path-length difference is less than one-half of the wavelength  $\lambda_1$ . As is well-known, the main contribution to the wavefield comes from the first FV as the rapid oscillatory responses of the higher-order FVs and Fresnel zones cancel out and give minor contributions to the wavefield (Born & Wolf, 1999). That is why in our work we restrict ourselves to the first FV which will be simply referred to as FV.

The IFZ is defined as the cross section of the FV by an interface which may not be perpendicular to the geometrical ray SMR. If the source S and the receiver R are situated at the same distance from the interface, the IFZ is represented by an ellipse centered at the reflection point M, whose equation is obtained from the formulation of the ellipsoid of revolution, eq.3, keeping the sign + and replacing  $z$  by  $z_M$ . The in-plane semi-axis  $r^{\parallel}$  and the transverse semi-axis  $r^{\perp}$  of the IFZ are then expressed as:

$$r^{\parallel} = \left[ \frac{\lambda_1}{2} \left( \frac{z_M}{\cos\theta} + \frac{\lambda_1}{8} \right) \right]^{\frac{1}{2}} \left[ 1 - \frac{z_M^2 \tan^2\theta}{\left( \frac{z_M}{\cos\theta} + \frac{\lambda_1}{4} \right)^2} \right]^{-\frac{1}{2}} , \quad r^{\perp} = \left[ \frac{\lambda_1}{2} \left( \frac{z_M}{\cos\theta} + \frac{\lambda_1}{8} \right) \right]^{\frac{1}{2}} \quad . \quad (4)$$

The characteristics of the IFZ depend on the positions of the source-receiver pair, and also on the incidence angle of the geometrical ray SMR. Moreover, larger portions of the interface (reflector) are involved for low-frequency than for high-frequency components of the wavefield. It is also well-known that a perturbation of the medium actually affects the reflected wave when this perturbation is located inside the IFZ.

Expressions for the semi-axes of the IFZ associated with the reflected wavefield, given by eq.4, are identical to those reported in Kvasnicka & Cerveny (1996a). Nevertheless, contrary to Kvasnicka and Cerveny, we state that they are exact for all incidence angles  $\theta$ , even in the critical and postcritical regions, where reflected wave and head wave interfere. Each wave has its own IFZ with different characteristics (Kvasnicka & Cerveny, 1996b), and in these regions, only wavefields interfere, not IFZs. In fact, the purposes in using the FV representation described above, instead of the classical representation of the FV by an ellipsoid of revolution with foci at the receiver R and at the mirror image S' of the source S, are twofold. First, for the case of a reflector with a curvature quite identical to that of the FV described above, the part of reflector involved in the reflected wavefield is greater in this representation than in the classical one (Figure 1). This fact is in good agreement with observations about the size of the IFZ for syncline-type reflectors (Lindsey, 1989). Second, for the case of an interface with lateral change in physical properties, this representation allows the definition of a volume of integration and partial homogenization of properties above and beyond the “mathematical” interface, which is necessary to evaluate an effective reflectivity of the reflector (Favretto-Cristini et al., Submitted to Geophysics Letters).

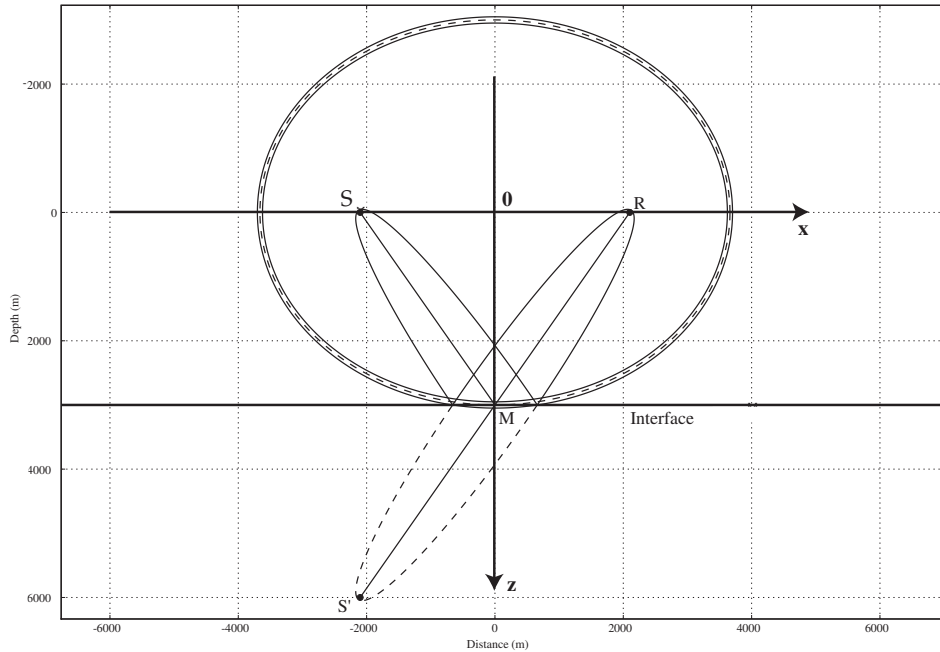


Figure 1: Representation, in the  $(\vec{x}, \vec{z})$ -plane, of the Fresnel volume involved in the wave reflection at the point M at a plane interface, under the incidence angle  $\theta = 35^\circ$ . The source S and the receiver R are situated at a distance 3000 m from the interface. The image source is denoted by S'. The velocities of the upper and lower media are respectively  $V_{P1} = 4000\text{m/s}$  and  $V_{P2} = 4300\text{m/s}$ , and the frequency  $f = 32\text{Hz}$ . The seismic wavelengths in the upper and lower media are respectively  $\lambda_1 = 125\text{m}$  and  $\lambda_2 = 134\text{m}$ .

## 1.2 Analytical expression for the reflected P-wave amplitude

We consider the same previous configuration. Let the orthotropic source be located at the point S, far from the plane interface between two homogeneous isotropic elastic media. The spherical P-wave emanating from the source propagates obliquely in the upper medium and strikes the interface. It is then reflected from the interface and finally recorded at the receiver located at the point R, far from the interface. Our objective is to calculate the amplitude of the reflected P-wave measured at the receiver, by accounting for the FVs and the IFZ which physically contribute to the wave propagation process.

The problem under consideration can be viewed as a problem of diffraction by the physically relevant part of the interface (namely, the IFZ). We chose to apply the Angular Spectrum Approach (ASA) (Goodman, 1996) to get the 3D analytical solution to this problem. The motivations of this choice are twofold. First, provided the incident spherical wavefield is decomposed by Fourier analysis into a linear combination of elementary plane wavesurfaces, traveling in different directions away from the source, the effect of propagation over distance is simply a change of the relative phases of the various plane wavesurface components. Second, Sherman (Sherman, 1967) has proved that despite their apparent differences, the ASA and the first Rayleigh-Sommerfeld solution (Goodman, 1996, chapter 3 page 47) yield identical predictions of diffracted fields. The advantage of using the ASA then seems obvious : it permits straightforward derivations of the measured amplitude of the reflected wave at the point R. We refer to the book of Goodman (Goodman, 1996, chapter 3 pages 55-61) for a detailed treatment of the ASA.

As mentioned above, the source wavefield is first decomposed by Fourier transform operation into a collection of elementary plane wavesurfaces traveling in different directions away from the point source. When using the ASA, we have to remind that it is a technique for modeling the propagation of acoustic fields between parallel planes.

Therefore, considering the case of the reflection of fields from an oblique interface requires several stages (Belgroune et al., 2002) including rotations. Nevertheless, in the case of the reflection by an interface the ASA can be used without rotations by simply considering a propagation from the mirror image of the source to the receiver as a transmission-like process.

Across the plane perpendicular to the specular ray passing through  $z = z_M$ , the amplitude  $U$  generated by the point source  $S$  and diffracted by the IFZ has a two-dimensional Fourier transform given by :

$$A(f_x, f_y, z_M, \theta) = \int \int_{-\infty}^{+\infty} U(x, y, z_M, \theta) \exp[-j2\pi(f_x x + f_y y)] dx dy \quad (5)$$

where  $U(x, y, z_M, \theta) = \frac{e^{ikR_M}}{R_M} H_F(x, y, \theta)$  with  $R_M = \sqrt{x^2 + y^2 + z_I^2}$  and  $z_I = z_M / \cos \theta$

The function  $H_F(x, y, \theta)$  represents the size of the IFZ which is a function of the incidence angle  $\theta$  :

$$\begin{cases} H_F(x, y, \theta) = 1 & \text{if } (x, y) \in IFZ \\ H_F(x, y, \theta) = 0 & \text{if } (x, y) \notin IFZ \end{cases}$$

$A(f_x, f_y, z_M, \theta)$  represents the plane-wave decomposition of the incident wavefield i.e., the angular spectrum. As indicated in (Goodman, 1996), the direction cosines of each plane wave associated with the frequencies  $(f_x, f_y)$  are given by

$$\alpha = \lambda f_x \quad \beta = \lambda f_y \quad \gamma = \sqrt{1 - \alpha^2 - \beta^2}$$

As the incident wavefield is reflected from the interface, the angular spectrum of the resulting wavefield is obtained by multiplying  $A(f_x, f_y, z_M, \theta)$  by the classical plane wave reflection coefficient  $R(f_x, f_y, \theta)$ , given by Zoeppritz equations (Aki & Richards, 2002). This coefficient takes into account the fact that the central ray is incident on the interface under the incidence angle  $\theta$ .

$$A_R(f_x, f_y, z_I, \theta) = A(f_x, f_y, z_I, \theta) R(f_x, f_y, \theta) \quad (6)$$

The resulting angular spectrum is propagated to the parallel plane passing through the receiver :

$$A_R(f_x, f_y, z_R, \theta) = A_R(f_x, f_y, z_I, \theta) \exp[j2\pi\gamma z_I/\lambda] \quad (7)$$

and by inverse transform, we get the amplitude :

$$U(x, y, z_R, \theta) = \int \int_{-\infty}^{+\infty} A_R(f_x, f_y, z_R, \theta) \exp[j2\pi(f_x x + f_y y)] dx dy \quad (8)$$

Since the receiver is located at the center of the plane, the amplitude of the reflected wavefield recorded at the receiver is finally given by  $U(0, 0, z_R, \theta)$

## 2 Comparison with the exact solution and with the plane-wave theory prediction

The aim of this section is to emphasize the importance of using the band-limited data concept, based on the IFZ, in order to simulate the amplitudes of the reflected waves recorded at receivers. For this purpose, it is instructive to compare the variation in the amplitude obtained with our approximation (ASA combined with the FV and IFZ concepts), as a function of the incidence angle, with the amplitude predicted by a numerical code which provides the exact solution, and with the amplitude predicted by the classical PW theory (here, the Zoeppritz equations (Aki & Richards, 2002)). We used the 3D code OASES to compute accurately synthetic seismograms in media. OASES is a general purpose computer code for modeling seismo-acoustic propagation in horizontally stratified media using wavenumber integration in combination with the Direct Global Matrix solution technique (Schmidt & Jensen, 1985; Schmidt & Tango, 1986; Jensen et al., 1994). In seismology, the wavenumber integration methods are often referred to as reflectivity methods or discrete wavenumber methods (Fuchs & Muller, 1971; Bouchon, 1981; Kennett, 1983; Olson et al., 1984; Muller, 1985). This software has the great advantage of providing reference solutions for various types of sources (explosive source, vertical point force, etc...). In addition, upward and downward propagation of compressional and of shear waves can be easily separated. This 3D code is widely used in the underwater acoustics community and has been thoroughly validated.

One case of interface between elastic media whose properties are reported in Table 1 has been chosen to illustrate the theoretical results. The interface is situated at a distance  $z_M = 3000m$  from the source-receiver plane. The amplitude  $U_0(f)$  is chosen to be the Fourier transform of a Ricker wavelet with the dominant frequency  $f = 16 Hz$  (respectively,  $f = 32 Hz$ ) and the frequency bandwidth  $B = 16 Hz$  (respectively,  $B = 10 Hz$ ).

Figure 2 depicts the amplitude-versus-angle (AVA) curves provided by the exact solution, by our approximation, and by the PW theory. The geometrical-spreading compensation was applied to the predictions of our 3D approximation, and to the synthetic data provided by the 3D code OASES, in order to be compared in a suitable way with the PW predictions.

Properties	$V_P$ (m/s)	$V_S$ (m/s)	$\rho$ (kg/m <sup>3</sup> )
Upper medium	4000	2000	2000
Lower medium	4300	2100	2200

Table 1: Properties of the homogeneous, isotropic, and elastic media in contact.  $\rho$ ,  $V_P$  and  $V_S$  denote, respectively, the density, P-wave and S-wave velocities for the upper (subscript 1 in the text) and lower (subscript 2 in the text) media.

Both curves were then normalized by the ratio  $\frac{R(\theta=0)}{U(\theta=0)}$ , where  $R(\theta=0)$  is the PW reflection coefficient calculated for the normal incidence, whereas  $U(\theta=0)$  is the amplitude obtained with either our approximation, or the numerical code, for the normal incidence. Inspection of Figure 2 shows that for subcritical angles, both AVA curves are quite identical. As the PW reflection coefficient varies smoothly with the incidence angle, the geometrical-spreading compensation is sufficient to reduce the amplitude of the reflected wave generated by the point source to the reflected plane-wave amplitude. For this type of interface with low impedance contrast, the effect of the IFZ on the wave amplitude is negligible for the subcritical region. On the contrary, in the vicinity of the critical angle, which is about  $68.5^\circ$  in the case of interest here, the PW reflection coefficient rapidly increases with the incidence angle, and the geometrical-spreading compensation is not sufficient anymore. Therefore, the additional application of the FV and IFZ concept becomes necessary.

In Figure 2, we can also note that just below the critical angle, the predictions of our approximation fit well the exact solutions. Nevertheless, with increasing incidence angle, the approximate solutions show increasing discrepancies in comparison with the exact solutions. The explanation comes from the fact that we calculate only the reflected wave amplitude, whereas the code OASES provides the amplitude of the interference between the reflected and the head wavefields. The contribution of each wavefield to the global amplitude recorded at the receiver cannot be discriminated in the synthetic seismograms, because both waves have the same traveltimes for a specific range of incidence angles. For great postcritical angles, for which the signal relative to the head wave and the signal relative to the reflected wave could be separated in time, our approximations should tend to the exact solutions. Unfortunately, the numerical computations for the ASA and for the code OASES could not be performed for such great incidence angles, because they are too CPU time-consuming. In fact, it would be more interesting to get the amplitude of the head wave by using the combination of the ASA with the IFZ concept associated with this particular wave, in order to sum up the amplitude of the reflected wave and that of the head wave, taking into account the phase shifts. This would enlighten on the complex physical process of wave interference with the reflected wave. Our present work is focused precisely on this particular aspect and will be reported later.

Figure 2 illustrates that the curves associated with the exact solutions exhibit oscillations above the critical angles, which suggests the imprint of the IFZ on the wave amplitudes. Even if they do not perfectly fit the exact curves, our approximations have got a similar behaviour. The amplitude of the oscillations decreases with increasing incidence angles, which is in good agreement with the fact that they may result from the interference of the IFZ with the sharp edge of the reflection coefficient.

Finally, note the peculiar effect of the frequency bandwidth of the source signal on the reflected wave amplitudes provided by the code OASES. For a given dominant frequency of the source spectrum, the larger the frequency bandwidth, the more quickly attenuated the

amplitude of the oscillations. Both the dominant frequency and the frequency bandwidth are therefore important for modeling of seismic wave propagation.

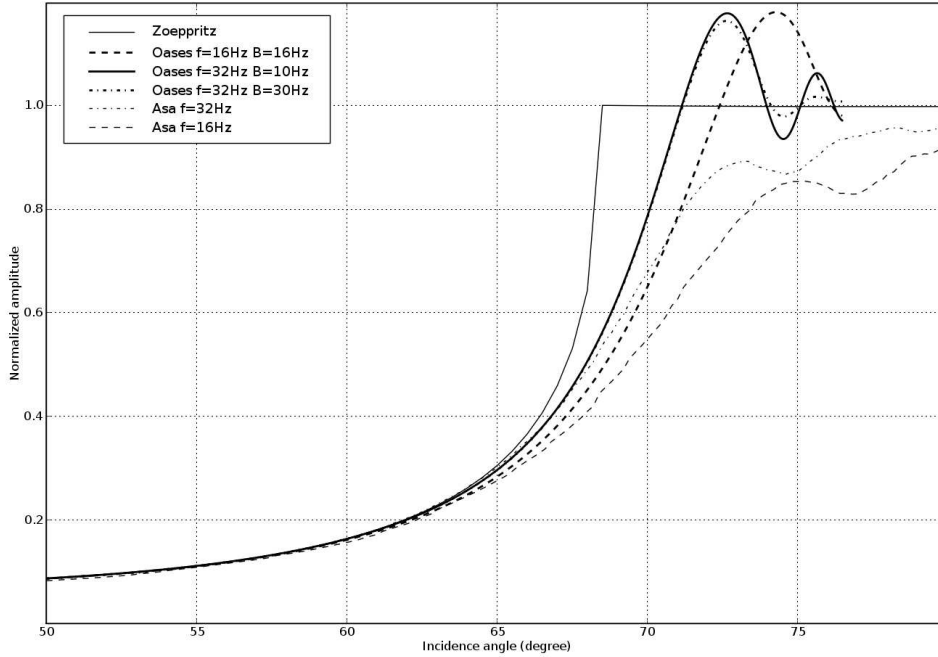


Figure 2: Variation of the amplitude of the P-wave reflected from a plane interface, as a function of the incidence angle. Comparison between the plane-wave reflection coefficient and the spreading-free amplitudes associated with the exact solution and with the approximate solution. The exact solutions are provided by the 3D code OASES, whereas the approximate solutions are obtained by applying the Angular Spectrum Approach together with the Interface Fresnel Zone concept.

## Conclusion

The aim of the paper was to discuss the usefulness of accounting for the Fresnel volume (FV) and for the Interface Fresnel Zone (IFZ) for simulating the amplitude of the P-wave emanating from a point source and recorded at a receiver after its specular reflection on a smooth interface between two elastic media. First, we have reformulated the concept of the FV by accounting for all possible rays defining the isochrone for the source-receiver pair and the specular reflected wave, in order to derive the expression for the IFZ valid whatever the incidence angle. As the problem under consideration can be viewed as a problem of diffraction by the IFZ, i.e. the physically relevant part of the interface which actually affects the reflected wavefield, we have then applied the Angular Spectrum Approach (ASA) to get the 3D analytical solution. The variation in the reflected P-wave amplitude, as a function of the incidence angle, evaluated with the ASA combined with the IFZ concept, has been compared with the plane-wave reflection coefficient, and with the exact solution obtained with the 3D code OASES. It results that

for some typical configurations and for subcritical incidence angles, the geometrical-spreading compensation is mostly quite sufficient to reduce the point-source amplitudes to the PW amplitudes. On the contrary, for critical and post-critical incidence angles, this compensation is not sufficient anymore, and the additional application of the FV and IFZ concept becomes necessary. Moreover, as our approximation is concerned only with the reflected wave, its predictions fit well the exact solution, provided there is no interference between the reflected wave and the head wave. For a further validation of our method, we need to evaluate the amplitude of the head wave by taking into account its own IFZ. Nevertheless, our predictions exhibit a behaviour similar to that of the exact solution, and particularly oscillations in the postcritical regions which illustrate the imprint of the interference between the IFZ and the sharp edge of the reflectivity of the interface. We have also shown on the exact solution curve that both the dominant frequency and the frequency bandwidth of the source signal have important effect on seismic wave propagation.

## Acknowledgments

We are grateful to two anonymous reviewers whose relevant suggestions helped us to improve the present paper significantly.

## References

- Aki, K. & Richards, P., 2002. *Quantitative seismology*, University Science Books, 2nd edn.
- Belgroune, D., de Belleval, J., & Djelouah, H., 2002. Modelling of the ultrasonic field by the angular spectrum method in presence of interface, *Ultrasonics*, **40**, 297–302.
- Born, M. & Wolf, E., 1999. *Principles of Optics*, Cambridge University Press, 7th edn.
- Bouchon, M., 1981. A simple method to calculate Green's functions for elastic layered media, *Bull. seism. Soc. Am.*, **71**, 959–971.
- Cerveny, V., 2001. *Seismic Ray Theory*, Cambridge University Press, Cambridge, UK.
- Cerveny, V. & Soares, J., 1992. Fresnel volume ray-tracing, *Geophysics*, **57**(7), 902–915.
- Dahlen, F. & Baig, A. M., 2002. Fréchet kernels for body wave amplitudes, *Geophys. J. Int.*, **150**, 440–466.
- Dahlen, F., Hung, S.-H., & Nolet, G., 2000. Fréchet kernels for finite-frequency traveltimes-i. theory, *Geophys. J. Int.*, **141**, 157–174.
- Favier, N. & Chevrot, S., 2003. Sensitivity kernels for shear wave splitting in transverse isotropic media, *Geophys. J. Int.*, **153**, 213–228.
- Fuchs, K. & Muller, G., 1971. Computation of synthetic seismograms with the reflectivity method and comparison of observations, *Geophys. J. R. astr. Soc.*, **23**, 417–433.
- Goodman, J., 1996. *Introduction to Fourier Optics*, MacGraw-Hill, 2nd edn.

- Hubral, P., Schleicher, J., Tygel, M., & Hanitzch, C., 1993. Determination of fresnel zones from traveltimes measurements, *Geophysics*, **58**(5), 703–712.
- Jensen, F., W.A. Kuperman, M. P., & Schmidt, H., 1994. *Computational Ocean Acoustics*, American Institute of Physics, New York.
- Kennett, B. L. N., 1983. *Seismic wave propagation in stratified media*, Cambridge University Press, Cambridge.
- Knapp, R., 1991. Fresnel zones in the light of broadband data, *Geophysics*, **56**(3), 354–359.
- Kravtsov, Y. & Orlov, Y., 1990. *Geometrical optics of inhomogeneous media*, Springer Series on Wave Phenomena, Springer-Verlag, NY.
- Kvasnicka, M. & Cerveny, V., 1994. Fresnel volumes and fresnel zones in complex laterally varying structures, *J. Seism. Explor.*, **3**, 215–230.
- Kvasnicka, M. & Cerveny, V., 1996. Analytical expressions for fresnel volumes and interface fresnel zones of seismic body waves. part 1: Direct and unconverted reflected waves, *Stud. Geophys. Geod.*, **40**, 136–155.
- Kvasnicka, M. & Cerveny, V., 1996. Analytical expressions for fresnel volumes and interface fresnel zones of seismic body waves. part 2: Transmitted and converted waves. head waves, *Stud. Geophys. Geod.*, **40**, 381–397.
- Lindsey, J., 1989. The fresnel zone and its interpretative significance, *The Leading Edge*, **8**(10), 33–39.
- Marquering, H., Dahlen, F., & Nolet, G., 1999. Three-dimensional sensitivity kernels for finite-frequency traveltimes: the banana-doughnut paradox, *Geophys. J. Int.*, **137**, 805–815.
- Muller, G., 1985. The reflectivity method: a tutorial, *J. Geophys.*, **58**, 153–174.
- Olson, A., Orcutt, J., & Fisher, G., 1984. The discrete wavenumber/finite element method for synthetic seismograms, *Geophys. J. R. astr. Soc.*, **77**, 412–460.
- Schleicher, J., Hubral, P., Tygel, M., & Jaya, M., 1997. Minimum apertures and fresnel zones in migration and demigration, *Geophysics*, **62**, 183–194.
- Schmidt, H. & Jensen, F., 1985. A full wave solution for propagation in multilayered viscoelastic media with application to Gaussian beam reflection at fluid-solid interfaces, *J. Acoust. Soc. Am.*, **77**, 813–825.
- Schmidt, H. & Tango, G., 1986. Efficient global matrix approach to the computation of synthetic seismograms, *Geophys. J. R. astr. Soc.*, **84**, 331–359.
- Sheriff, R., 1980. Nomogram for fresnel-zone calculation, *Geophysics*, **45**(5), 968–972.
- Sherman, G., 1967. Application of the convolution theorem to rayleigh’s integral formulas, *J. Opt. Soc. Am.*, **57**, 546.
- Spetzler, J. & Snieder, R., 2004. The fresnel volume and transmitted waves: a tutorial, *Geophys. J. Int.*, **69**(3), 653–663.

- Vasco, D. & Majer, E., 1993. Wavepath traveltime tomography, *Geophys. J. Int.*, **115**, 1055–1069.
- Vasco, D., Peterson, J. J., & Majer, E., 1995. Beyond ray tomography: wavepaths and fresnel volumes, *Geophysics*, **60**(6), 1790–1804.
- Yomogida, K., 1992. Fresnel zone inversion for lateral heterogeneities in the earth, *Pure Appl. Geophys.*, **138**(3), 391–406.
- Zhou, Y., Dahlen, F., Nolet, G., & Laske, G., 2005. Finite-frequency effects in global surface-wave tomography, *Geophys. J. Int.*, **163**, 1087–1111.